

Simulation of the Flow Pattern Around Spur Dykes Using FLUENTS

Othman A. Karim
K.H.M. Ali

ABSTRACT

The ultimate objective of this study is the prediction of flow pattern associated with spur dykes. Prediction of velocity fields and bed shear stresses were obtained using the FLUENT package. The RNG k- ϵ formulation in FLUENT has been validated against selected benchmark solutions of flow in the vicinity of spur dykes. Extensive testing procedures have been implemented to ensure that the equations and solution algorithms used by FLUENT would provide an accurate simulation of flow. Experiments carried out by Mayerle et al. (1995) and Zaghoul and McCorquodale (1975) were selected as benchmark for verification purposes. FLUENT predicted reasonably well the attachment point downstream of the dyke in the flat-bed case. Calculated bed shear stresses can then be used in appropriate sediment continuity equations for the prediction of scour hole geometries.

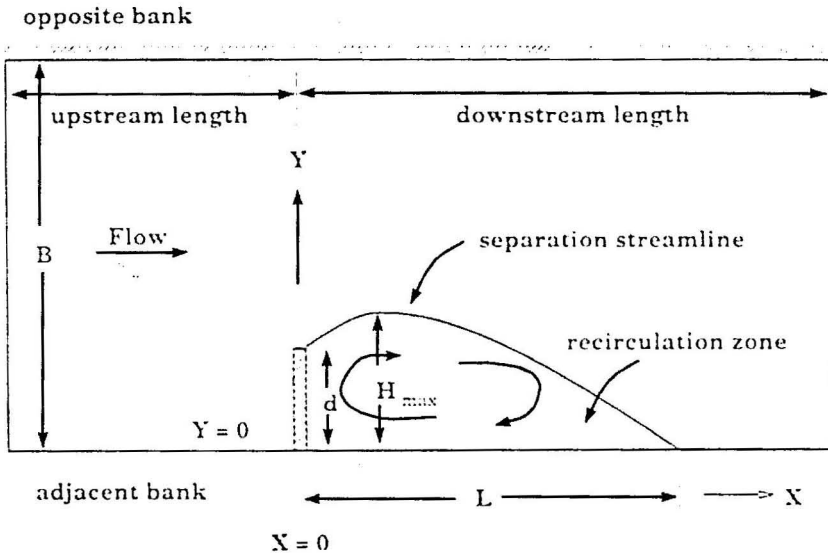
ABSTRAK

Objektif akhir kajian ini ialah ramalan bentuk corak aliran dan tegasan ricih berkaitan dengan struktur tambak taji. Ramalan medan halaju dan tegasan ricih diperolehi menggunakan perisian FLUENT. Formula RNG k- ϵ yang terdapat di dalam FLUENT telah disahkan menggunakan pilihan ujian tanda aras penyelesaian aliran di sekeliling tambak baji. Tatacara ujian secara extensif dilakukan bagi memastikan persamaan-persamaan serta algoritma penyelesaian yang digunakan di dalam FLUENT memberikan penyelakuan aliran yang tepat. Ujikaji-ujikaji yang telah dijalankan oleh by Mayerle et al. (1995) dan Zaghoul and McCorquodale (1975) telah dipilih sebagai ujian tanda aras bagi tujuan pentahkikan. FLUENT meramalkan dengan agak baik titik pelekatan di hilir tambak baji bagi kes dasar rata. Nilai tegasan ricih yang dikira seterusnya boleh digunakan dalam persamaan keselantaran enapan bagi meramalkan geometri lubang kerukan.

INTRODUCTION

The problem of scour around any obstruction placed in alluvial channel is of great importance to hydraulic engineers. In practise, a channel is often obstructed by one means or the other. Such structures, when introduced to a flow channel, result in significant changes to the flow pattern. Detailed description of the modified flow, due to the obstruction, is essential to understanding and analysis of the local scour that develops. This paper will examine one type of such structure, known as a spur-dyke, or sometimes

referred to as a groyne. Schematic layout of typical channel and spur-dyke arrangement is shown in Figure 1 (Othman 1996).



Spur-dykes are hydraulic structures with one end adjacent to the bank and the other end projecting into the main flow. They are constructed mainly to: (1) protect river banks against erosion; (2) train the river along a desired course by attracting, deflecting or repelling the flow in the channel; (3) create a slack flow with the objective of silting up the area in the vicinity; and (4) create local scour holes and provide stable, submerged stony substrate for habitat improvement (Mayerle et al. 1995). The most important aspects to be considered in their design are the layout, plan view, shape, length, spacing, crest longitudinal shape, crest elevation, orientation, permeability, construction materials, bed material and local scour. The majority of these aspects can nowadays be examined with numerical models. Numerical model simulations are usually more cost-effective and faster than physical model studies, and have no inherent limitation on spatial extent. This paper is therefore aimed at investigating the capability of the FLUENT package in simulating the flow in the vicinity of spur dykes.

REVIEW OF RELEVANT PAST WORKS

It is not intended here to give any detailed review of literature on the spur-dykes problem. However, a brief reference to several works relevant to the present analysis is made. Numerical models capable of simulating the flow near a spur dyke are rare. Zaghloul and McCorquodale (1973, 1975) developed such a model solving the Helmholtz vorticity equation and Poisson-type equation. Tingsanchali and Maheswaran (1987) simulated the flow around a spur dyke by solving the 2D, depth averaged equations with a $k-\epsilon$ turbulence model. Their results agreed with the experimental data only after a streamline curvature factor was applied to the $k-\epsilon$ model. More recently, Mayerle et al. (1995) simulated the flow near spur dykes using a

3D numerical model developed at the Center for Computational Hydroscience and Engineering in Oxford, USA. Comparisons were made between six eddy viscosity approaches. The results were also compared with measurements carried out at the Franzius Institute in Hannover, Germany.

One of the major difficulties in simulating flows numerically in the vicinity of spur dykes or bridge piers, is the inadequate reproduction of the wake or secondary flow formed downstream. The proper reproduction of the wake length is of fundamental importance to the design of dykes since it defines the length of the protected bank and thus the spacing between subsequent dykes. Some work, although not as much as piers related problems, has been done about various aspects of the hydraulic characteristics of spur-dykes. Laboratory measurements (Garde et al. 1961) show that the wake length is affected by the ratio of the dyke length to the channel width, the angle between the dyke centre line and the current, and the flow depth. It is also influenced by the bottom roughness which generates smaller wake length in the field. Contrary to expectations, Barbarutsi et al. (1989) concluded from their investigations that Froude number has little influence on the wake length.

In numerical model simulations, the wake length is strongly influenced by the eddy viscosity field (Othman 1996; Mayerle et al. 1995). The full development of mathematical models as reliable engineering tools is, at present, hindered by the lack of an acceptable theory for the mixing coefficients especially on the horizontal plane. Even though algebraic models have been successfully applied to predict certain types of near parallel flows and different geometric configurations, usually a different model needs to be formulated and modified for each individual type of flow. The use of more sophisticated turbulence models is not always the answer to the problem, since in addition to more equations to be solved and inherent difficulties in using these models, some of them are based on local velocity gradients. Furthermore, other uncertainties in the simulation in rivers and coastal areas regarding the exact bathymetry and bottom boundary conditions whenever sediment transport is included hardly justifies the use of more advanced models. The main purpose of this study is to investigate the suitability of the existing FLUENT code to compute and analyse the flow velocity patterns in the vicinity of a spur dyke.

FLUENT VALIDATION

Velocity results obtained from a numerical model and experimental work reported by Mayerle et al. (1995) are used as benchmarks to validate the effectiveness of the FLUENT numerical model in simulating flows in the vicinity of the dykes. Subsequently, the FLUENT package is used to predict the flow field and bed shear stress over a scoured bed caused by a spur dyke, as obtained by Zaghoul and McCorquodale (1975) .

THE WORKS OF MAYERLE ET AL. (1975)

Mayerle et al. simulated the flow near spur dykes using a 3D numerical model developed at the Center for Computational Hydroscience and Engineering in Oxford, USA. The model was based on the solution of time-

dependent nonlinear Navier Stokes equations, the kinematic condition of the free surface, and the continuity equations respectively for the velocities in the horizontal plane, the surface elevation, and the vertical velocity. A numerical methodology named Efficient Element Technique which combines the advantages of both finite element and finite difference method was employed. In their study, Mayerle et al. (1995) compared results from six different eddy viscosity turbulence approaches with measurements carried out at the Franzius Institute in Hannover, Germany. The measurements were carried out in a 32.4 m long by 2.5 m wide concrete flume with a horizontal bottom and a Manning's coefficient of 0.02. The rectangularly shaped spur dyke normal to the main flow direction was 0.25 m long and 0.05 m thick. Velocity profiles along the longitudinal and transversal directions at eleven positions near the dyke, and cross-sectional velocity measurements in the circulation region were carried out using an ultrasonic current meter. The measurements were carried out for a flow with a discharge of 200 l/s and a depth of 0.23 m over a period of 102.4 seconds. A reattachment length equal to 2.88 m ($11.5d$, d being the dyke length), was observed.

Fluent Simulation The hydrodynamic system of the physical model described above, was represented by a 3-dimensional finite volume grid system of $40 \times 20 \times 10$. Time dependence model was activated with time increment, Δt set to 0.01 secs. In general, it is desirable to increase grid resolution in regions where the flow variables exhibit large gradients. For the spur dykes problem, the area around the spur and the recirculation zone qualify as high-gradient regions; consequently, the grid spaces was closer near the spur, near the sidewall to which the spur was attached and near the bottom. The simulated domain and the grid system are shown in Figure 2. The inlet and outlet boundaries were placed respectively 1.5 m upstream and 3.0 m downstream of the spur-dyke. These distances were considered appropriate to avoid disturbances due to the presence of the dyke. Uniform velocity of $0.08 \text{ m}^2/\text{s}$ was assigned to the inlet boundary. At the bottom, the roughness coefficient (ELOG) was calculated based on an equivalent roughness height of 0.0023 m. The free surface was modelled as slip boundary.

Results and Discussions The quasi-steady state three-dimensional conditions were obtained after 120 secs (12,000 iterations) whereby the normalised residuals reported by FLUENT are almost constant. This is consistent with the number of iteration reported by Mayerle et al. (1995) Figures 3 - 5 show the velocity vectors and corresponding bed shear stresses for $t = 40, 80$ and 120 secs, respectively, for model rng. The recirculation zone downstream of the dyke in the numerical model results was defined as the region in which the longitudinal velocities are in opposite direction to the main flow direction. This region is represented by the contours of negative velocity behind the dyke as depicted in Figures 3 - 5.

Figures 6 compare longitudinal velocity profiles at six positions (cross section A,B, and C - refer Figure 2), between the FLUENT results, Mayerle et al. (1995) model results and the physical model measurements. It can be seen from the figures that none of the simulated results (FLUENT and Mayerle's models) agrees systematically with the measurements. Mayerle et al. argued that at the dyke tip (position A3) the results vary significantly

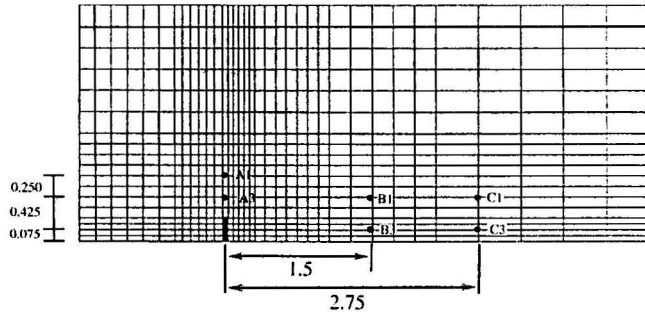
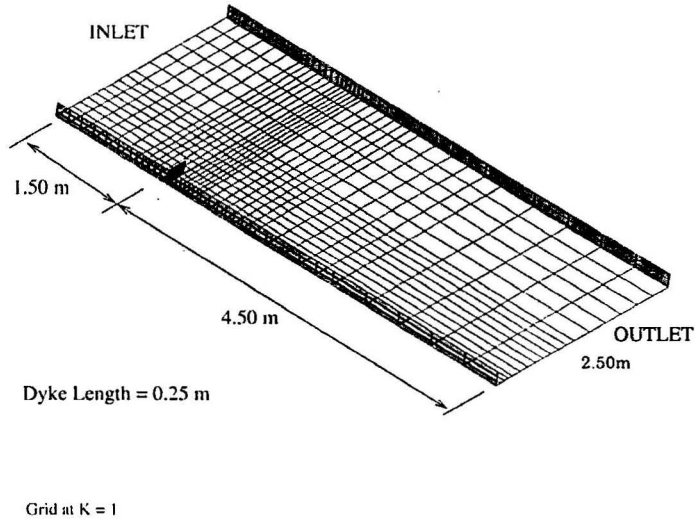
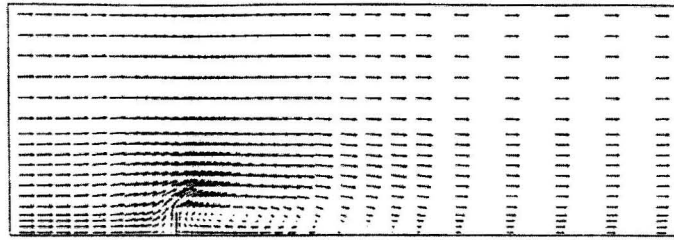


FIGURE 2. Simulated domain and grid-system in FLUENT

from the measurements. This is probably due to the locally non-hydrostatic pressure. Downstream of the dyke and outside the recirculating region (position B1 and C1), both FLUENT and Mayerle's model are not able to capture the decrease in the longitudinal velocities towards the free surface shown by measurements. However, FLUENT predicts the velocity better in this region compared to Mayerle's approaches. Figure 7a and 7b shows comparisons of the longitudinal velocities near the bed along two cross sections of the channel. The cross sections are taken as 0.338 m (section D) and 1.55 m (section E) downstream of the dyke axis. FLUENT's result fit reasonably well within the range of results obtained by Mayerle et al.

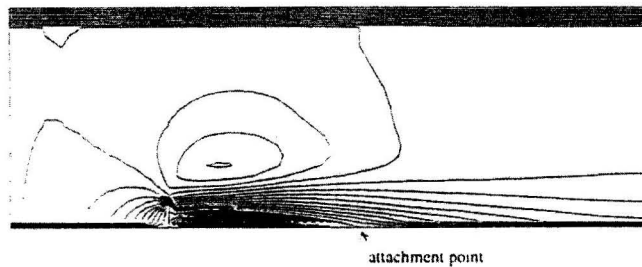
The reattachment point was taken as a point where separation of flow occurs at the wall boundary. It can be seen from Figures 3 - 5 that the recirculation zone, hence the attachment point, increases with time. For the present analysis, reattachment length at quasi-equilibrium stage ($T=120\text{secs}$) was found to be 2.74 m ($\approx 11d$), downstream from the dyke axis. This compared very well with the value obtained from the physical model (2.88 m or $11.5d$). Mayerle, et al. [2] reported reattachment lengths ranging from $8.4d$ to $15.2d$, the nearest being $10.8d$. Independent studies by Francis et al. (1968) and Ishii et al. (1983) reported reattachment lengths approximately

(a) Velocity Vectors

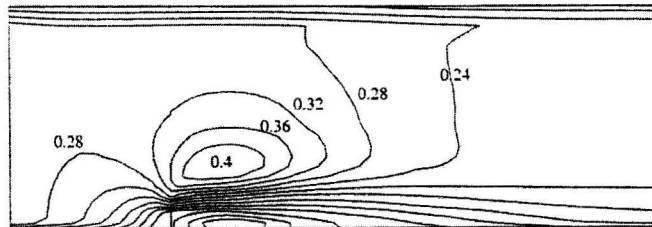


→ 0.40 m/s

(b) U-Velocity Contours



(c) X-Dir Bed Shear Stresses



Contours Interval : 0.04 Pa

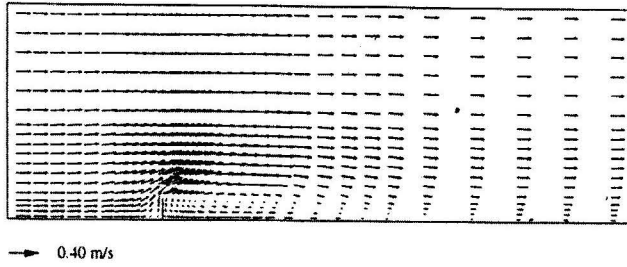
FIGURE 3. FLUENT Output ($t = 40$ secs)

equal to $11.5d$ for dykes placed perpendicularly to the main flow direction having a ratio of dyke length to channel width equal to 0.1. Francis et al. carried out their measurements in a 0.46 m wide rectangular cross section channel using groyne lengths of 0.023 m, 0.0509 m and 0.080 m whereas Ishii et al. (1983) used two laboratory flumes (0.8 m and 0.396 m wide) to investigate the effect of some dimensionless properties on the shape of separation formed behind dykes.

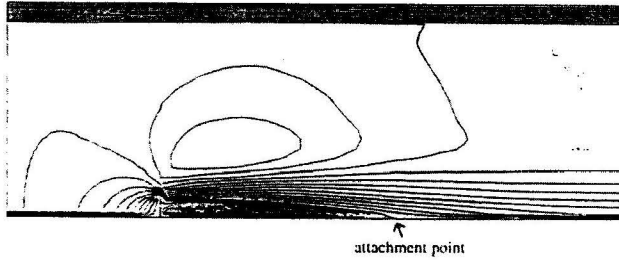
THE WORKS OF ZAGHLOUL AND MCCORQUODALE (1973, 1975)

Zaghloul and McCorquodale (1973) developed a numerical model for local scour prediction around a single spur dyke. They also conducted experiments to verify their mathematical model. The clear-water scour experiments were carried out in a rectangular channel of width 45.75 cm, containing a sand

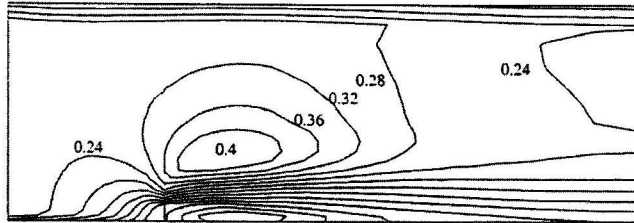
(a) Velocity Vectors



(b) U-Velocity Contours



(c) X-Dir Bed Shear Stresses



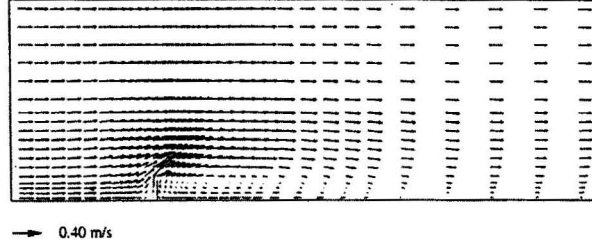
Contours Interval : 0.04 Pa

FIGURE 4. FLUENT Output (t = 80 secs)

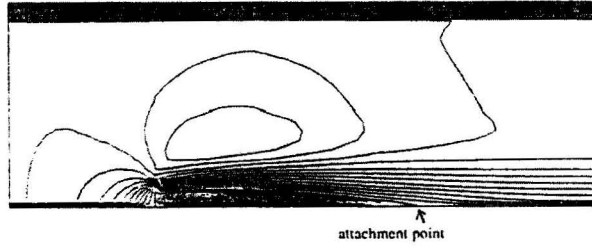
bed with a mean particle diameter of 4.5 mm. The specific gravity and the angle of repose for the bed material are respectively 2.65 and 30°. The critical shear stress on a level bed for the sediments were found experimentally to be approximately 3.6 Pa. Several flow conditions were investigated and scour patterns were monitored, to determine the effect of the following parameters on the maximum depth of scour: (1) flow rate, (2) upstream water depth, (3) opening ratio, i.e. ratio of width of channel at spur dyke to width of channel upstream, (4) Froude number upstream of spur dyke, (5) angle of inclination of spur dyke to the flow, and (6) running time. Typically, duration of 3 hours is observed before limiting scour condition was reached. They suggested an empirical shear stress equation, which was generated from the computed local velocity, turbulence and vorticity, and has the form:

$$\tau_b = \frac{\gamma}{C^2} v_r^2 \left(1 + K_1 \frac{\omega}{\omega_0} + K_2 \right)^2 \quad (1)$$

(a) Velocity Vectors



(b) U-Velocity Contours



(c) X-Dir Bed Shear Stresses

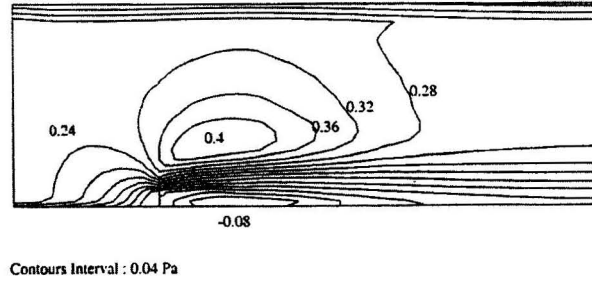


FIGURE 5. FLUENT Output (t = 120 secs)

in which τ_b is the shear stress acting on the bed, γ is the specific weight of water, C is Chezy coefficient, v_R is the resultant velocity, K_1 and K_2 are constants and ω_0 is a reference vorticity e.g. the vorticity at the nose of the dyke. Adjustments were made to the calculated eroded depth so that the final computed scour profile conformed to the condition that the local shear equalled the bed resistance. An expression controlling the development of the scour hole was formulated as:

$$\Delta z = K_3 (\tau - \tau_{sc}) \quad (2)$$

where Δz is the increment in the eroded bed, K_3 is the constant, and τ_{sc} is the critical shear stress for the bed material taking into account the local bed slope. It was however not clear how they calculated the value of the τ_{sc} . They obtained an excellent agreement between theoretical and experimental

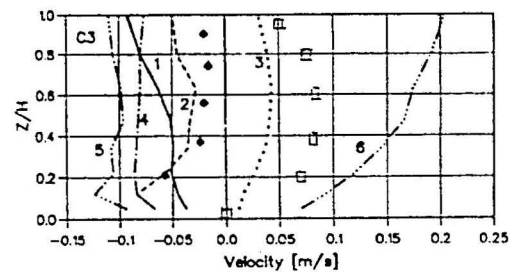
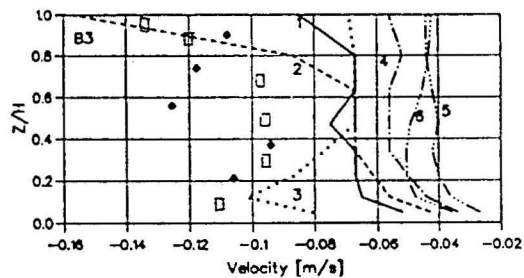
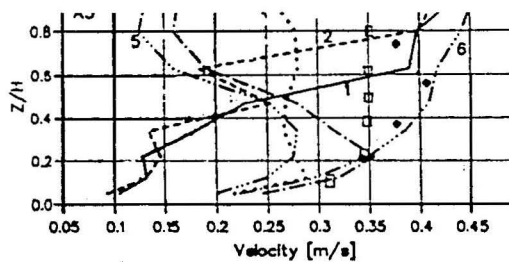
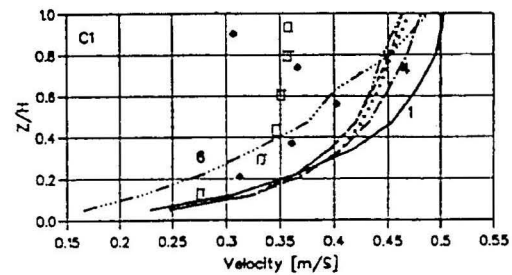
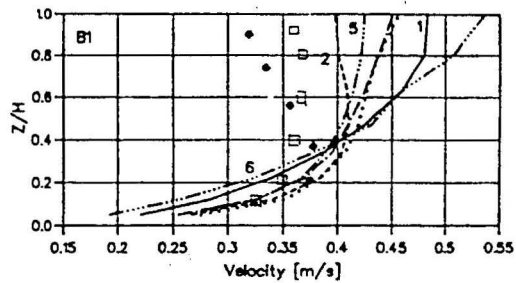
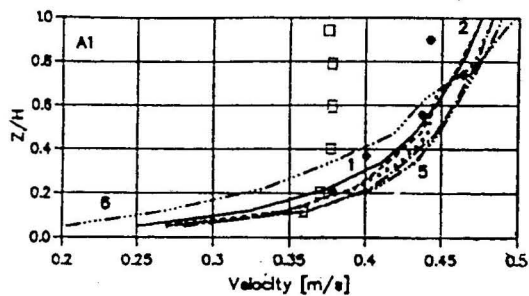


FIGURE 6. Comparisons of longitudinal vertical velocity profile
 (- FLUENT, Experimental, 1-6: Mayerle et al.'s models

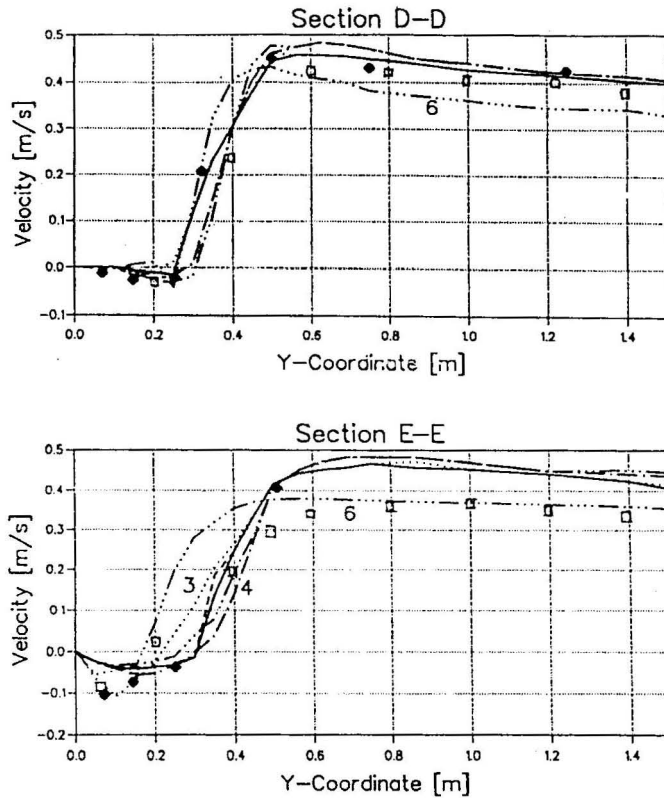


FIGURE 7. Cross sectional plots of the longitudinal velocities downstream of spur-dyke (Section D-D: 0.338m; Section E-E: 1.55m downstream
(□ - FLUENT, ♦ Experimental, 1-6: Mayerle et al.'s models)

scour patterns. The calculated and experimental scour pattern for the flow condition with an average upstream velocity and water depth of 40.87 cm/s and 20.32 cm, respectively, are shown in Figure 8.

Fluent Simulation The time development of scour represents a very complicated flow phenomenon involving the movement of sediment-water mixture along the bed of the scour hole. The existence of structure such as spur-dyke that obstruct the flow adds to the complexity of the problem. The accelerated flow at the tip of the structure combined with the vortices and the shear stress at the bed are among major factors that lead to extensive erosion in the vicinity of the spur-dyke. Due to the continuously changing flow boundary as scour progresses with time, the velocity distribution pattern in the scour hole would likewise be different at different stages of the erosion process. In the present study, no attempt was made to simulate these transient non-uniform flow patterns. Instead a steady-state flow model was simulated based on the initial flat bed condition, and final scoured pattern as observed by Zaghoul and McCorquodale (1975).

The opening ratio, α , defined as $(B-d)/B$ (B being the width of the channel and d being the length of the spur dyke) is equal to 0.67. A uniform velocity of 0.4087 m/s was applied at inlet boundary. The outlet boundary

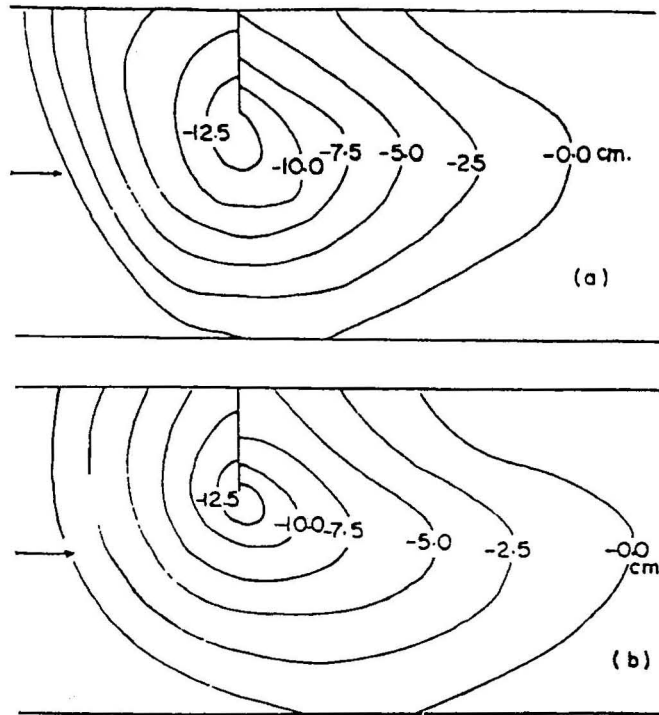


FIGURE 8. (a) Experimental and (b) Computed Scour Pattern, after Zaghoul and McCarquodale (1975).

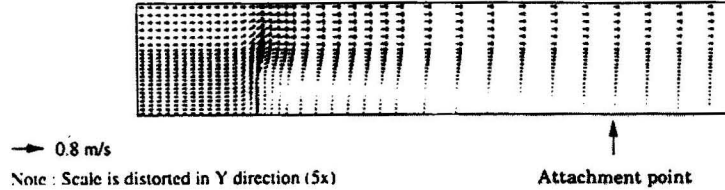
was first located at $40d$, a distance greater than the expected attachment point. Initial trial runs for rigid-bed case indicated that this distance was not appropriate, as the flow at the exit does not reach steady-state. This distance was then increased to $80d$, and was found to be appropriate for practical computational purposes. In addition, several grid arrangements were tried to ensure that the results were independent of grid size distribution. A three-dimensional grid size of $70 \times 25 \times 12$ was used in the simulation.

RESULTS AND DISCUSSIONS

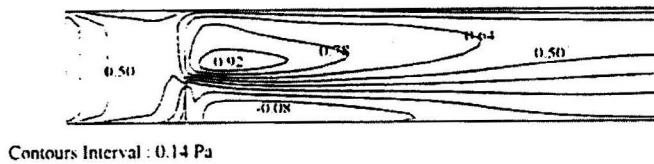
Figure 9(a) and 9(b) show the computed steady-state velocity vectors plots and resulting bed shear stress respectively for flatbed. It can be seen from these figures that with an opening ratio, α , of 0.67, the attachment length, L , is equal to $37.3d$, almost four times greater than the distance obtained in the previous study (i.e. $11d$ for opening ratio of 0.9). Another run with shorter spur-dyke length (Figure 10) with the opening ratio of 0.78 resulted in shorter attachment length ($L = 15.3d$). Tingsanchali and Maheswaran (1987) and Francis et al. (1968) observed the same trend in which the distance L increases with the decreases in the opening ratio. Tingsanchali and Maheswaran (1987) further reported from their numerical analysis that beyond a certain length of the spur-dyke, the presence of the opposite wall limits the growth of the recirculation width, H_{\max} (Figure 1), and thus the length of recirculating zone.

(a) Velocity Vectors

Width of Channel : 0.46 m

Spur length, $d = 15$ cmSpur Width, $w = 3.5$ cm

(b) X-Dir Bed Shear Stresses



(c) Y-Dir Bed Shear Stresses

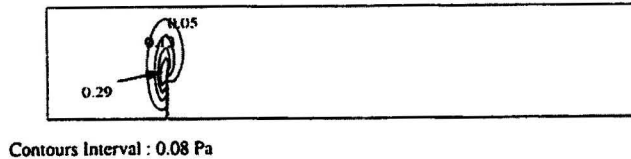
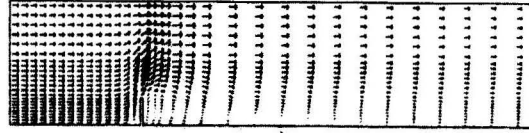


FIGURE 9. FLUENT output (flatbed)

Figure 10(c) shows that the attachment distance for a run of a spur-dyke with dimensions $W = 1.5$ cm, is smaller than a wider spur-dyke with the same opening ratio (≈ 0.67). The attachment length, L , in this case was calculated to be $30.3d$ from the dyke axis. This preliminary results indicate the importance of the spur shape, for instance in determining the spacing of spurs. Unfortunately no experimental data are available for comparison in this case.

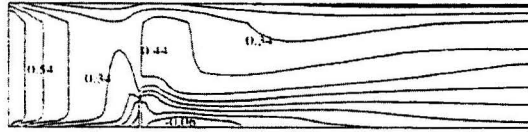
As the water flows around the spur-dyke, the flow pattern is changed due to the reduction of the width of channel. As a result of this, the shear distribution around the spur-dyke is modified. This leads to scouring action until equilibrium is established between various forces influencing the scouring action. In almost all cases, the maximum scour depth occurred at the nose of the spur-dyke. The scour hole upstream of the spur-dyke was conical in shape, whereas downstream, it was elongated and had a shallower shape (Garde et al. 1961). Experimental work carried out by Rajaratnam and Nwachukwu (1983), using 75 mm and 150 mm groynes, observed that the shear stress near the groyne was higher for the smaller opening ratio. They also indicate that the results for the

Width of Channel : 0.46m
 Spur Length, d = 10 cm
 Spur Width, W = 3.5 cm

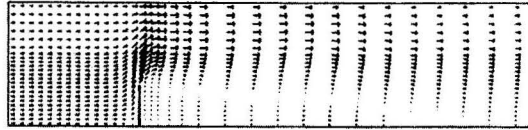


Attachment point

Bed Shear Stress



Width of Channel : 0.46m
 Spur Length, d = 15 cm
 Spur Width, W = 1.5 cm



Attachment point

FIGURE 10. Effect of changing spur-dyke geometry
 (scale distorted in y direction (5x))

75 mm groyne for which the opening ratio is 0.92, might represent the asymptotic case, i.e., the opening ratio for which the effect of constriction on the channel flow farther away is negligible. The result exhibited by FLUENT (Figure 10) is consistent with this finding. Similarly, Garde et al. (1961) and Zaghloul and McCorquodale (1975) showed that the scour hole increases as the opening ratio decreases. Zaghloul formulated an empirical equation, based on the experimental findings, to illustrate the degree of dependence of the scour depth on various influencing factors. This equation is given by:

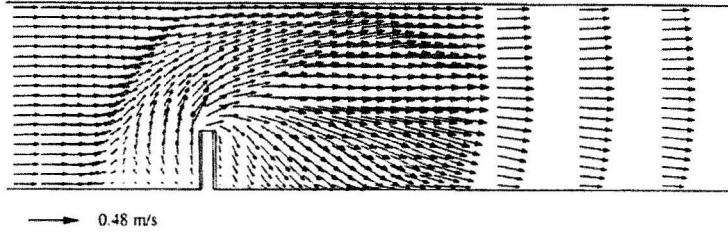
$$\frac{D_s}{H} = 2.62(F)^{2/3} \left(\frac{1}{\alpha} \right) \left(\frac{1}{\theta} \right)^{0.043} \quad (3)$$

where D_s = maximum depth of scour, F = Froude number, α = opening ratio and θ = angle of inclination of the spur-dyke with respect to the main flow.

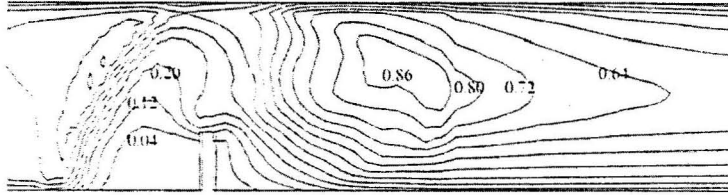
Garde et al.(1961) proposed an equation given as:

$$\frac{H+D}{H} = \left(\frac{K}{\alpha} \right) F^{2/3} \quad (4)$$

(a) Velocity Vectors (at bed)

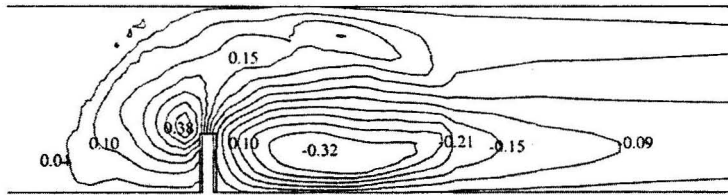


(b) X-Dir Bed Shear Stresses



Contours Interval : 0.08 Pa

(c) Y-Dir Bed Shear Stresses



Contours Interval : 0.06 Pa

FIGURE 11. FLUENT output (scoured bed)

where H = average depth of water flow. The above equation was derived for angle of inclination $\theta = 90^\circ$.

Zaghloul and McCorquodale (1975) suggested that allowances in the numerical models need to be made to account for the shedding mechanisms of vortices and the increased shear resulting from the horseshoe vortex in the vicinity of the dyke. They proposed an empirical equation (Eq. 1) which took into account the effect of the vortices. Roger (1994), on the other hand, adopted the bed shear stress formulated by Melville and Raudkivi:

$$\tau_b = \frac{\rho f u_b^2}{8} \quad (5)$$

where ρ is the density of water, f is Darcy Weisbach friction factor and u_b is the velocity measured at bed. This equation may not be applicable in a strongly curved flow, such as spur-dyke and piers, since its simplicity does not take into account the swirling effect.

Similarly, FLUENT had not taken into account such factors in the determination of the bed shear stress. Consequently, the magnitude of the shear stress calculated by FLUENT, as shown in the Figure 9, were considerably less than critical shear stress for the material for flat bed ($\tau_c = 3.6$ Pa). The results obtained for scoured bed are essentially lower than the results obtained for rigid bed (Figure 11). This is because as scour hole developed, the length of eddy zone and intensity of eddy currents in it decreased. Velocities near the bed also decreased because of the increase in total water depth. In the downstream region of the hole, however, the decrease in depth between the bed and the 'fixed' water surface causes the flow to converge and causes the velocity to increase thus leading to higher bed shear stress.

CONCLUSIONS

The *rng k- ϵ* formulation in FLUENT has been validated against selected benchmark solutions of flow in the vicinity of spur dykes. Extensive testing procedures have been implemented to ensure that the equations and solution algorithms used by FLUENT would provide an accurate simulation of flow, in particular the grid-independent and the location of the outlet/exit boundary.

Overall, the FLUENT results are good in balance. FLUENT successfully verifies that when a dyke is placed in a channel, it causes a significant disturbance downstream to the flow for a short distance upstream and for a longer distance downstream. FLUENT predicted reasonably well the attachment point downstream of the dyke in the flat-bed case.

It can be concluded that the shape of the spur-dyke effects to some extent, the location of the attachment point as well as the distribution of the shear stress in the vicinity of the spur-dykes. It is therefore important for numerical simulation purposes that the geometrical shape of the spur-dyke to be input as accurately as possible.

In general it was shown, experimentally and numerically, that the maximum bed shear stress occurred near the dyke nose and the immediate neighbourhood of the dyke. Comparison between calculated bed shear stress and the experimental critical bed shear stress for the flat bed, however, indicated that FLUENT results are considerably lower. This may be due to the failure of FLUENT to include the effect of the vorticity in the determination of the bed shear stress.

Another shortcoming of the FLUENT is that the present code is not capable of simulating the changes in the water level. Reports by Mayerle et al. (1995) and Rajaratnam & Awachukwu (1983) have described the lowering of the free surface at the nose of the spur dyke and behind it which FLUENT had not been able to simulate.

NOTATIONS

B	Width of channel
C	Chezy coefficient
d	Dyke length
D_s	maximum depth of scour
f	Darcy Weisbach friction factor
F	Froude number
H	Upstream water depth
H_{max}	Recirculation width
K_1, K_2, K_3	Constants
u_b	Velocity measured at bed
v_R	Resultant velocity
W	Width of spur-dyke
α	Opening ratio = $(B-d)/B$
γ	Specific weight of water
Δt	Time increment (FLUENT calculations)
Δz	increment in eroded bed
θ	angle of inclination of the spur-dyke with respect to main flow
ρ	Density of water
τ_b	Shear stress acting on the bed
τ_c	Critical bed shear stress
ω_o	Reference vorticity e.g vorticity at the nose of the dyke

REFERENCES

- Barbarutsi, S. Ganoulis, J. & Chu, V. H. 1989. Experimental investigation of shallow recirculation flows, *J. of Hydraulic Engineering*, ASCE 115 (7).
- Francis, J.R., Pattanick, A. & Wearne, S. 1968. Observations of Flow Patterns Around Some Simplified Structures in Channels, Technical Note No. 8 *Proc. Inst. of Civil Engineers*. London.
- FLUENT *User's Guide*. Lebanon, New Hampshire: FLUENT Incorporated.
- Garde, R.J., Subramanya, D.K. & Nambudripad, K.D. 1961. Study of Scour Around Spur-Dikes, *J. of Hydraulic Division*, ASCE, 87 (HY 6).
- Ishii, C., Asada, H. & Kishi, T. 1983. Shape of separation region behind a Groyne of non-overflow type in rivers. *Proceedings of the 20 IAHR Congress*, Vol 2, 405-412. Moscow.
- Mayerle, R. Toro, F.M. & Wang, S.S.Y. 1995. Verification of a Three-Dimensional Numerical Model Simulation of The Flow in The Vicinity of Spur Dikes. *J. of Hydr Res.* ASCE 33 (2)
- Othman A. Karim. 1996. Prediction of two and three dimensionals turbulent flows. PhD Thesis, University of Liverpool, United Kingdom.
- Rajaratnam, N. & Nwachukwu, B.A. 1983. Flow near groin-like structures. *J. of Hydraulic Engineering*, ASCE 109 (3).
- Roger, J.W. 1994. Investigation of the flow pattern around a spur dyke using the FLUENT package. MSc Thesis, University of Liverpool, United Kingdom.
- Tingsanchali, T. & Maheswaran, S. 1987. 2D depth averaged flow computation near Groyne. *J. of Hydraulic Engineering*, ASCE 116(1).

- Zaghloul, N & McCorquodale, J.A. 1973. A numerical model for flow past a spur dyke. *Proceedings of the First Canadian Hydraulics Conference*, University of Alberta, Edmonton.
- Zaghloul, N. & McCorquodale, J.A. 1975. A stable numerical model for local scour. *J. of Hydr Res.*, ASCE 13(4).

Othman M. Karim
Department of Civil Structural Engineering
Universiti Kebangsaan Malaysia
43600 UKM, Bangi,
Selangor D.E Malaysia.

K.H.M. Ali
Senior Lecturer, University of Liverpool
P.O. Box 147
Brownlow St.
Liverpool L69 3BX, UK